Chapter

V

Role of elastic strain energy and Interfacial energy

V-1. Introduction

During a first-order phase transformation, a heterogeneous state appears, even though the initial and final states are single-phase. After the formation of the new phase nucleus, the transformation is manifested by the movement of the interface boundary between the two phases. The energy level of the interface boundary and its properties are determined by the atomic structure of the boundary (including the degree of disorder) and the difference in chemical composition between the adjacent phases. It is evident that the greater the difference in the atomic structure of the phases (including differences in interatomic distances and coordination) and the nature of the atoms, the higher the interface energy will be.

V-2. Total coherent, semi-coherent, and incoherent

In crystals, different phases can be distinguished by the crystallographic directions along which interatomic directions are coincident. Examples of complete coincidence (in all three directions) in the arrangement of atoms include the formation of ordered domains or when a phase arises from a solid solution, which is isomorphic to the matrix but differs in composition. In such cases, we can speak of total coherence between the lattice of the new phase and the old phase (see Figure V-1-a).

Differences in specific volumes (atomic radii and interatomic distances) lead to elastic deformation. Lattice mismatch (ε) during the growth of the new phase crystal can result in the formation of dislocations, which reduce this elastic deformation (see Figure V-1-b).

$$\varepsilon = \frac{(a_p - a_M)}{a_M} \qquad \text{(V-1-)}$$

a_p: is the lattice parameter of the precipitated phase
a_M: is the lattice parameter of the matrix

The formation of a coherent interface is influenced by the energy gain, which depends on the degree of lattice mismatch between adjacent phases (see Fig. V-1-a). In most phases, each atom has an optimal arrangement of nearest neighbors that results in low energy. However, at the interface, there is typically a change in composition, causing each atom to interact with incorrect neighbors across the interface. This mismatch increases the energy of the interface atoms and contributes to the overall interface energy, denoted as γ_{ch}. For a coherent interface, this is the primary contribution, i.e.:

$$\gamma_{(coherent)} = \gamma_{ch} \qquad \text{(V-2-)}$$

In general, coherent interfacial energies can be up to about 200 mJ/m². When the atomic spacing at the interface is not identical, coherence can still be maintained by applying stress to one or both lattices, as illustrated in Fig. V-1-(a). The resulting lattice distortions are referred to as coherency strains.

The strains associated with a coherent interface increase the total energy of the system. When the atomic mismatch or interfacial area becomes sufficiently large, it becomes energetically more favorable to replace the coherent interface with a semi-coherent interface, as shown in Fig. V-1-(b).

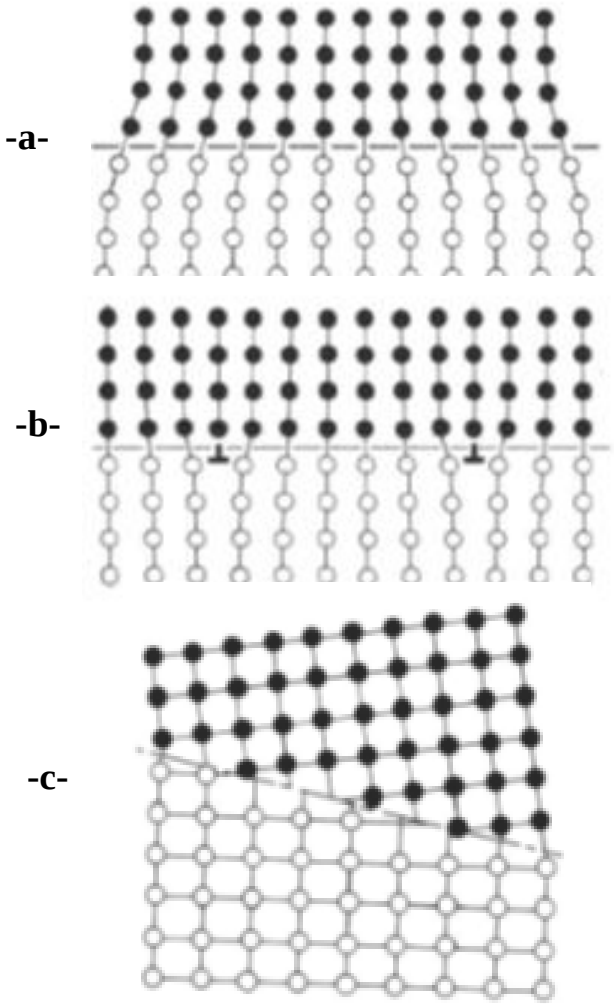

Fig. V-1-: Interfaces: (a) coherent (with a slight offset leading to coherence constraints in adjacent lattices), (b) semi-coherent, (c) incoherent

If d_α and d_β are the unconstrained interplanar spacings of the corresponding planes in the α and β phases, respectively (see Fig. V-2), the misfit between the two lattices is defined by:

$$\delta = \frac{d_\beta - d_\alpha}{d_\alpha} \qquad \text{(V-3-)}$$

It can be shown that, in one dimension, the lattice misfit can be fully compensated without generating a long-range strain field by introducing a set of edge dislocations with a distance DDD between them, given by:

$$D = \frac{d_\beta}{\delta} \qquad \text{(V-4-)}$$

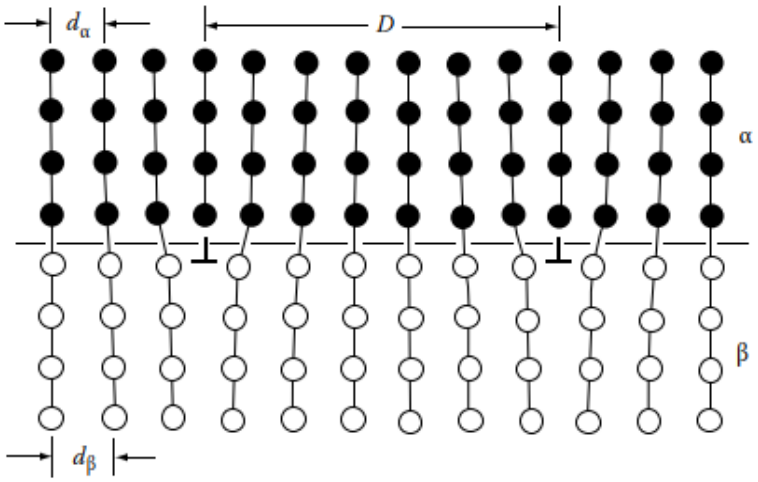

Fig. V-2-: Semi-coherent interface: The misfit parallel to the interface is compensated by a series of edge dislocations.

For small d,

$$D \cong \frac{b}{\delta} \qquad \text{(V-5-)}$$

Where b is the dislocation Burgers vector:

$$b = \frac{(d_\alpha + d_\beta)}{2} \qquad \text{(V-6-)}$$

The interfacial energy of a semi-coherent interface can be approximately viewed as the sum of two components: (a) a chemical contribution, γ_{ch}, similar to that of a fully coherent

interface, and (b) a structural term, γ_{st}, which represents the additional energy due to structural distortions caused by dislocations, i.e.:

$$\gamma_{\text{(semi-coherent)}} = \gamma_{ch} + \gamma_{st} \qquad \text{(V-7-)}$$

Equation (V-4) shows that as the shift δ increases, the spacing between dislocations decreases. For small values of δ, the structural contribution to the interfacial energy is approximately proportional to the dislocation density at the interface, i.e., for small δ, $\gamma_{st} \propto \delta$.

As the spacing between dislocations decreases, the associated strain fields increasingly overlap and cancel each other out. The energies of semi-coherent interfaces generally range from 200 to 500 mJ/m².

The introduction of additional dislocations disrupts the partial coherence, resulting in a completely incoherent interface (see Fig. V-1-c).

In general, incoherent interfaces occur when two randomly oriented crystals are joined along any interface plane, as shown in Figure V-1-c. However, they can also arise between crystals with an orientation relationship if the interface structure differs between the two crystals.

As the particles reach a sufficiently large size, lattice coherence is lost. The decrease in elastic energy is associated with the formation of accommodation dislocations at the grain boundaries.

Complete relaxation of elastic stresses is achieved once a sufficient number of dislocations have formed, such that the distance between them is:

$$l = \frac{b}{\varepsilon} \qquad \text{(V-8-)}$$

Where b is the Burger vector of the dislocations,

The mechanisms for the formation of dislocations can vary between different particles:

- Formation of prismatic loops around the particles within the matrix.
- Creation of dislocation loops inside the precipitates through the condensation of point defects.
- Generation of accommodation dislocations at the interface itself.

- Attraction of pre-existing dislocations from the matrix to the interface.

V-3- Characteristics of the phases formed by precipitation

The concepts of order, orientation relations, and coherence are crucial for describing the characteristics and properties of precipitates within a matrix.

A phase is considered *ordered* if its constituent atoms are arranged according to the geometric pattern of the crystallographic structure, with each crystallographic site occupied by a specific type of atom. This is known as long-range order. If there are fluctuations or deviations in the chemical assignment, the compound exhibits only short-range order. In the extreme case where atoms are arranged randomly on the crystallographic lattice, the phase is termed *disordered*.

Ordered precipitates typically consist of defined stoichiometric compounds with a restricted range of chemical compositions, which is characteristic of most equilibrium compounds. Metastable precipitates, which form during aging or tempering treatments, are often ordered.

Another important characteristic of structural precipitation is the nearly systematic presence of preferential crystallographic orientation relations between the matrix and the precipitates. These relations arise either from homogeneous precipitation or from heterogeneous precipitation on dislocations, sub-grain boundaries, or specific grain boundaries or phases within the matrix. This is particularly evident in epitaxial relations, where there is a parallel alignment between the crystallographic planes or directions of the matrix and those of the precipitates.

Finally, precipitates are considered coherent if there is geometric continuity between the crystallographic lattices of the matrix and the precipitates in all crystallographic directions. In this case, only the atomic arrangement within the lattice is altered (see Fig. V-3-a).

In aluminum alloys, coherent precipitation is the initial stage of homogeneous precipitation, occurring either during or after the formation of GP (Guinier-Preston) zones. Coherent precipitates are typically very small, generally up to 5 nm in size, unless the deviation from coherence is minimal. For GP zones, this deviation is relatively small, ranging from 0.1% to 1%.

When the coherence misfit is too high, dislocations become geometrically necessary at the precipitate-matrix interfaces to accommodate the elastic distortions. This mechanism is observed in precipitates with a significant coherence misfit, which is common in heterogeneous precipitation induced by crystallographic defects and can also result from the excessive growth of initially coherent precipitates. In such cases, the orientation relationships are semi-coherent, meaning that the lattice of the matrix and the precipitates are coherent only along a few specific planes or crystallographic directions (see Fig. V-3-b).

Finally, precipitates are considered incoherent if there is no specific crystallographic orientation relationship between the lattice of the matrix and that of the precipitate (see Fig. V-3-c). This represents the final stage of precipitation, typically resulting in equilibrium phases. An example of an incoherent precipitate is the θ ($CuAl_2$) phase in Al-Cu alloys. Although there is an orientation relationship between the θ precipitate and the aluminum matrix, this is likely due to the fact that θ forms from the θ' phase, rather than indicating that θ is semi-coherent with the matrix.

- **Precipitation at grain boundaries**

Particular situations arise when a second-phase particle is located at a grain boundary, as it requires considering the formation of interfaces with two differently oriented grains. Three possibilities can then occur (see Fig. V-4): (1) the precipitate may have incoherent interfaces with both grains, (2) it may have a coherent or semi-coherent interface with one grain and an incoherent interface with the other, or (3) it may have a coherent or semi-coherent interface with both grains. The first two cases are commonly encountered, while the third possibility is less likely.

The minimization of interfacial energy in these cases results in planar or slightly curved semi-coherent or coherent interfaces, and somewhat curved incoherent interfaces. An example of a grain boundary precipitate is shown in Fig. V-5.

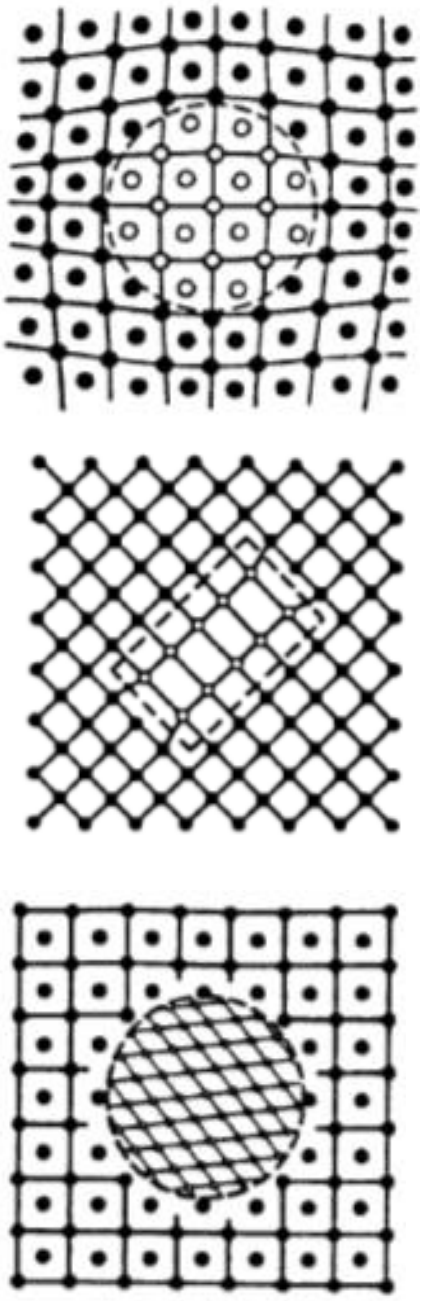

Fig. V-3- : (a) Coherent precipitate with lattice distortion due to volume variation
(b) Semi-coherent precipitate
(c) Incoherent precipitate

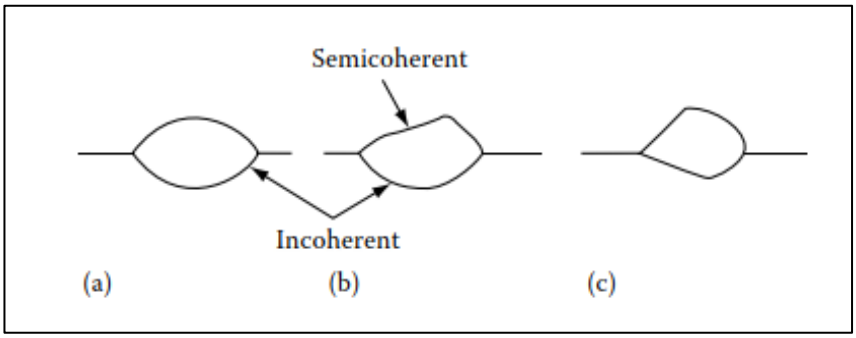

Fig. V-4-: Possible morphologies for grain boundary precipitates include:

- *Incoherent interfaces*: Slightly curved
- *Coherent or semi-coherent interfaces*: Planar

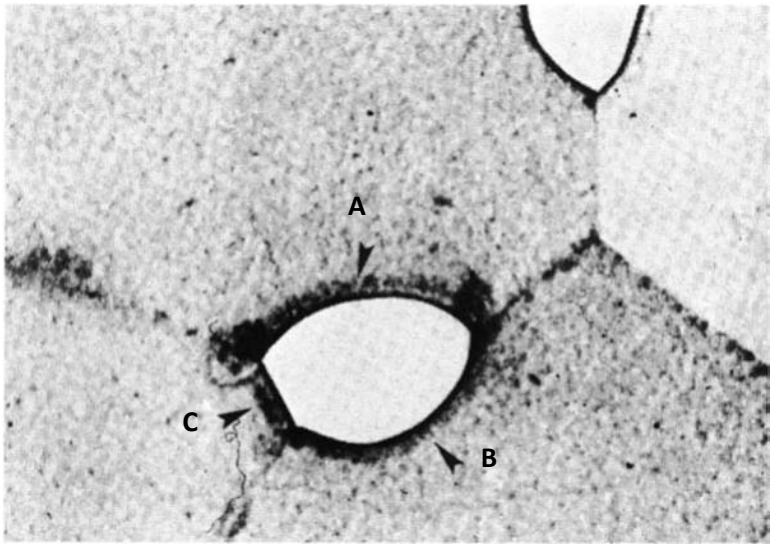

Fig. V-5-: A precipitate at a grain boundary triple point in an α-β Cu-In alloy, where interfaces A and B are incoherent, while interface C is semi-coherent (×310) *(After G.A. Chadwick, Metallography of Phase Transformations, Butterworths, London, 1972.)*

V-4- Misfit Strain effects

When a misfit is present, the formation of coherent interfaces increases the free energy of the system due to the elastic strain fields that develop. If this elastic strain energy is denoted as ΔGs, the equilibrium condition is given by:

$$\sum A_i \gamma_i + \Delta G_s = minimum \qquad \text{(V-9-)}$$

The origin of coherence constraints for a misfitting precipitate is illustrated in Fig. V-6. If the circled matrix volume in Figure V-6-(a) is sheared and the matrix atoms are replaced by

smaller atoms, the sheared volume will experience a uniform negative expansion strain toward an inclusion with a smaller lattice parameter, as shown in Figure V-6-(b). To achieve a fully coherent precipitate, the matrix and the inclusion must be subjected to equal and opposite strains, as depicted in Fig. V-6-(c).

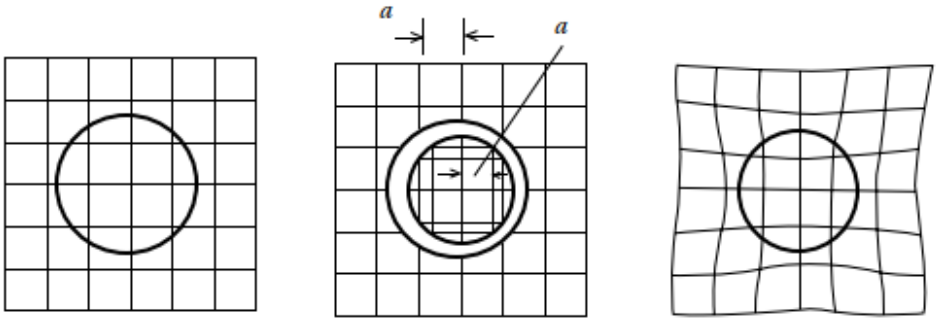

Fig. V-6-: The origin of coherence constraints.

If the lattice parameters of the unconstrained precipitate and the matrix are a_β and a_α, respectively, the unconstrained misfit δ is defined by:

$$\delta = \frac{a_\beta - a_\alpha}{a_\alpha} \qquad \text{(V-10-)}$$

However, the constraints that maintain coherency at the interfaces deform the lattice of the precipitate. For a spherical inclusion, this distortion is purely hydrostatic, meaning it is uniform in all directions, resulting in a new lattice parameter a_β'. The misfit with this constraint, denoted as ε, is defined by:

$$\varepsilon = \frac{a'_\beta - a_\alpha}{a_\alpha} \qquad \text{(V-11-)}$$

If the elastic moduli of the matrix and the inclusion are equal and the Poisson's ratio is 1/3, then ε and δ:

$$\varepsilon = \frac{2}{3}\delta \qquad \text{(V-12-)}$$

In practice, the inclusion typically has elastic constants different from those of the matrix; however, ε generally falls within the interval: $0.5\,\delta < \varepsilon < \delta$.

When the precipitate is a thin disk, the in-situ misfit is not uniform in all directions. Instead, it is relatively large perpendicular to the disk and nearly zero within the plane of the broad faces, as shown in Figure V-7.

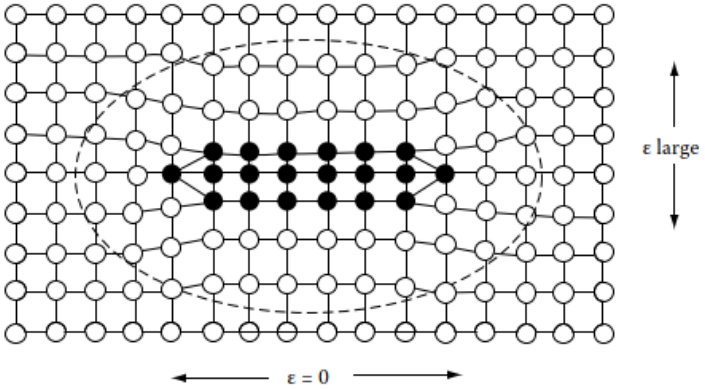

Fig. V-7-: For a coherent thin disk, the misfit is minimal parallel to the plane of the disk, with the maximum misfit occurring perpendicular to the disk.

In general, the total elastic energy depends on the shape and the elastic properties of both the matrix and the inclusion. However, if the matrix is elastically isotropic and the precipitate and matrix have equal elastic moduli, the total elastic strain energy ΔGs is independent of the precipitate's shape. Assuming a Poisson's ratio υ =1/3, it is given by:

$$\Delta G_s \cong 4\mu\delta^2 V \qquad \text{(V-13-)}$$

Where μ is the shear modulus of the matrix and V is the volume of the unstressed precipitate in the matrix. Therefore, the coherence strains generate an elastic strain energy that is proportional to the volume of the precipitate and increases with the square of the lattice misfit (δ^2).

When the inclusion is incoherent with the matrix, there is no effort to align the two lattices, and the lattice sites are not maintained across the interface. In such cases, there are no coherence constraints. However, misfit strains can still occur if the inclusion is not the correct size for the space it occupies (see Fig. V-8). In this scenario, the lattice shift δ\deltaδ is not significant, and it is more appropriate to consider the volume shift Δ, defined by:

$$\Delta = \frac{\Delta V}{V} \qquad \text{(V-14-)}$$

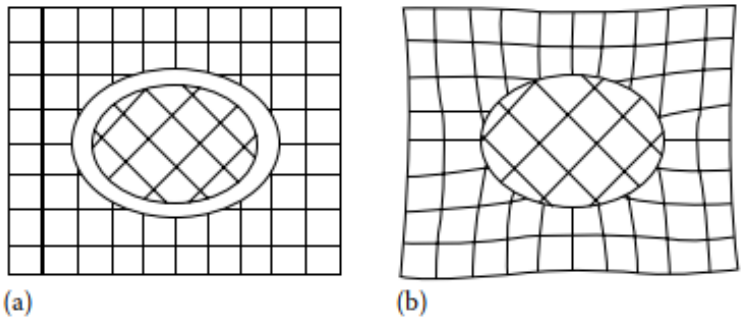

Fig. V-8-: The origin of misfit strain for incoherent inclusion

Nabarro provides the elastic strain energy for a homogeneous, incompressible inclusion in an isotropic matrix as:

$$\Delta G_s = \frac{2}{3}\mu\Delta^2 V f\left(\frac{c}{a}\right) \qquad \text{(V-15-)}$$

Where μ is the shear modulus of the matrix.

Thus, the elastic strain energy is proportional to Δ^2. The function f(c/a) accounts for shape effects and is illustrated in Fig. V-9. For a given volume, a sphere (c/a=1) has the highest strain energy, while a thin, flattened spheroid (c/a→0) has very low strain energy. A needle-like shape (c/a→∞) has strain energy between the two extremes. Therefore, the equilibrium shape of an incoherent inclusion will be an oblate spheroid with a c/a value that balances the competing effects of interfacial energy and strain energy. When Δ is small, the effects of interfacial energy should dominate, leading the inclusion to be approximately spherical.

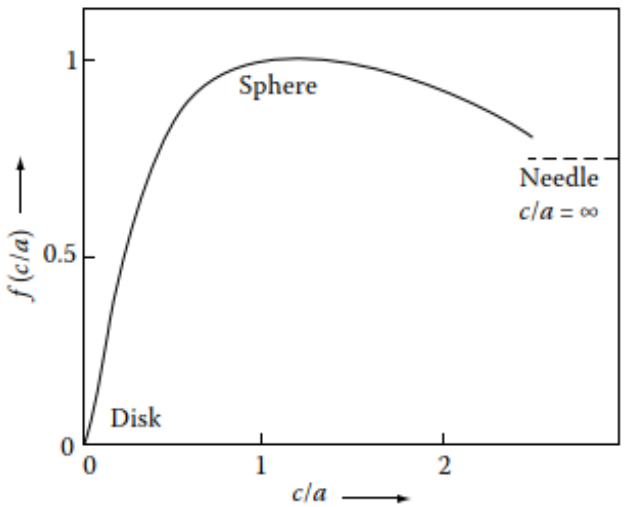

Fig. V-9- : The variation of f(c/a). *(After F.R.N. Nabarro, Proceedings of the Royal Society A, 175 (1940) 519.)*

V-5- Loss of coherence

Precipitates with coherent interfaces exhibit low interfacial energy, but they are associated with coherent strain energy in the presence of misfit. Conversely, if the same precipitate has non-coherent interfaces, it will exhibit higher interfacial energy. Now, consider which state yields the lowest total energy for a spherical precipitate with misfit δ and radius r.

The free energy of a crystal containing a fully coherent spherical precipitate includes contributions from:

- The coherence strain energy, described by the following equation,
- The interfacial chemical energy γ_{ch}.

The sum of these two terms is given by:

$$\Delta G_{coh} = 4\mu\delta^2 \frac{4}{3}\pi r^3 + 4\pi r^2 \gamma_{ch} \qquad \text{(V-16-)}$$

If the same precipitate has incoherent or semi-coherent interfaces, there will be no mismatch energy, but there will be an additional structural contribution to the interfacial energy γ_{st}. The total energy in this case is given by:

$$\Delta G_{non-coh} = 0 + 4\pi r^2(\gamma_{ch} + \gamma_{st}) \qquad \text{(V-17-)}$$

For a given δ, $\Delta G_{(coherent)}$ and $\Delta G_{(non\text{-}coherent)}$ vary with r as shown in Fig. V-10. When small, the coherent state provides the lowest total energy, while for large precipitates, it is more favorable for them to be semi-coherent or incoherent (depending on the magnitude of δ). At the critical radius (r_{crit}); $\Delta G_{(coherent)} = \Delta G_{(non\text{-}coherent)}$, giving:

$$r_{crit} = \frac{3\gamma_{st}}{4\pi\delta^2} \qquad \text{(V-18-)}$$

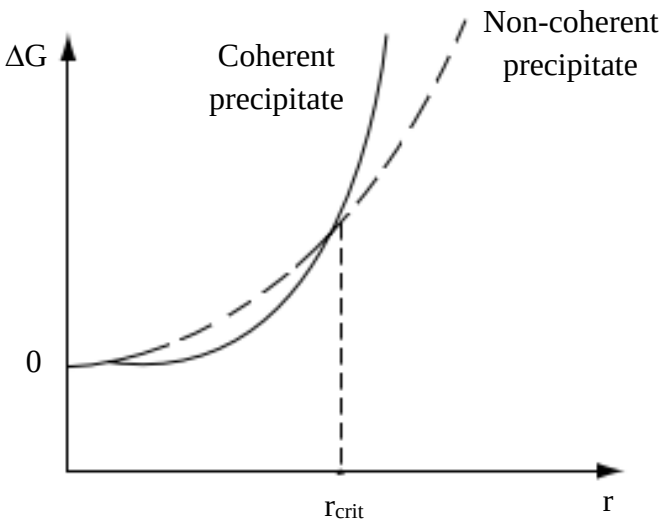

Fig. V-10-: Total energy of the matrix plus precipitate as a function of the radius of the precipitate, for both coherent and non-coherent spherical precipitates (semi-coherent or incoherent).

- **Characteristics of the phases formed during precipitation and their modulated structure**

These structures are formed, for example, during the demixing of solid solutions. In binary alloys such as Ni-Al, Ni-Ti, Ni-Au, and ternary alloys like Cu-Ni-Fe and Fe-Ni-Al, two new isomorphic phases with different compositions are formed. The dependence of the lattice parameter on the concentration follows Vegard's law:

$$a = a_0(1 + q_0 C) \qquad \text{(V-19-)}$$

Where:

a_0 is the lattice parameter of one of the constituents.

q_0 is the expansion coefficient of the lattice.

C is the concentration of the 2nd component.

Differences in composition and thus in lattice parameters inevitably lead to the imposition of constraints. It can be demonstrated that, in terms of elastic energy, the formation of complexes consisting of alternating lamellae—enriched and depleted in one of the elements—is more favorable than the formation of separate phases in the form of independent discs.

Practice exercises

Exercise 1:

Mg can dissolve in Al to form a substitutional solid solution. However, Mg atoms are larger than Al atoms, and therefore each Mg atom distorts the surrounding Al lattice, creating a stress field that effectively exists around each Mg atom.

- Show the strain energy in kJ mol^{-1} and eV $atom^{-1}$.
- What hypotheses are implicit in this calculation?

We give: The shear modulus of μ_{Al} = 25GPa, r_{Al} = 1,43 Å, r_{Mg} = 1,60 Å.

Exercise 2:

Figure -1- shows the various phases, both stable and metastable, present in the Al-4 at.% Cu alloy. These phases are presented in the figure, not necessarily in the chronological order of their formation.

- Characterize the interfaces for each phase and indicate which phases are expected to germinate most easily. Deduce the hardening precipitation sequence in Al-Cu alloys.

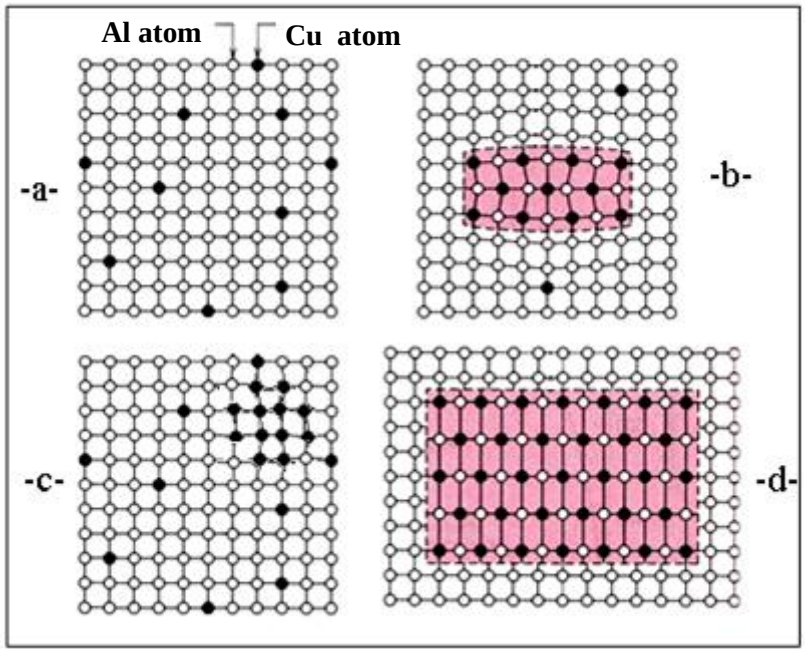

Figure 1

Exercise 3:

1. A coherent interface between a precipitate and a matrix is characterized by an interfacial energy γ_{ch}.
- What precipitate shape minimizes this surface contribution?
2. In reality, the lattice parameters of precipitates are not perfectly equal to the lattice parameter of the matrix, resulting in semi-coherent interfaces.
- What is the free energy associated with the presence of a spherical precipitate?
3. If the same precipitate has an incoherent (or semi-coherent) interface,
- What occurs?
- What is the free energy associated with the presence of this precipitate in this case?
4. For a given misfit δ, illustrate the variation of ΔG_{coh} and ΔG_{incoh}.
- What do you observe?

Answers

Answers for Exercise 1

$\Delta G_s \cong 4\mu\delta^2 V$

δ=0.119

V=1.225x10^{-29} m^3

μ_{Al} = 25 GPa=25x10^9 Nm^{-2}

ΔG_s = 10.5 kj.mol^{-1} = 0.1 eV.atom^{-1}

It is also implicitly assumed that individual Mg atoms are sufficiently spaced apart so that each atom can be considered isolated, i.e., in a dilute solution. The use of Equation 3.39 also relies on the assumption that the matrix surrounding a single atom behaves as a continuum.

Answers for Exercise 2

- GP zones are coherent with the matrix (fig. -3-c-).
- θ’ precipitates are semi-coherent with the matrix (fig. -3-b-).
- θ precipitates are incoherent with the matrix (fig. -3-d-).

- The precipitation sequence:

$\alpha \rightarrow \alpha_1 + GP \rightarrow \alpha_2 + \theta'' \rightarrow \alpha_3 + \theta' \rightarrow \alpha_4 + \theta$

Answers for Exercise 3

1- The shape that minimizes this surface contribution is a sphere.
2- Elastic deformation is necessary to accommodate the atoms at the interface, resulting in additional energy due to this deformation.

The free energy associated with the presence of a coherent spherical precipitate consists of two contributions:

- the deformation energy: $\Delta G_{st} = 4/3\pi r^3 * 4\mu\delta^2$
- the interface energy: $\Delta G_{ch} = 4\pi r^2\gamma_{ch}$

$$\mathbf{\Delta G_{coh} = 4/3\pi r^3 * 4\mu\delta^2 + 4\pi r^2\gamma_{ch}}$$

In this case, the precipitate is much less deformed, making its deformation energy negligible. However, a second term, γ_{st}, is added to the interface energy, which then becomes:

$$\Delta G_{ch} = 4\pi r^2(\gamma_{ch} + \gamma_{st})$$

hus, the total free energy for an incoherent precipitate is: $\mathbf{\Delta G_{incoh} = 4\pi r^2(\gamma_{ch} + \gamma_{st})}$

3-

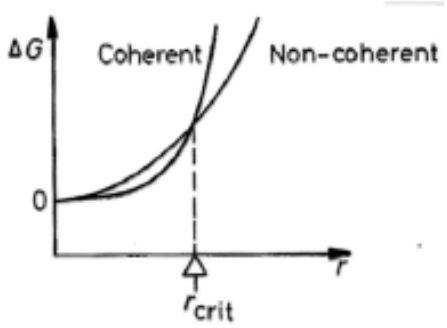

It is observed that a small precipitate is more favorably coherent, while a larger precipitate tends to be incoherent.